Vol. 15, No. 2 (2026): 676 - 688 http://dx.doi.org/10.23960/jtepl.v15i2.677-688

JURNAL TEKNIK PERTANIAN LAMPUNG

ISSN 2302-559X (print) / 2549-0818 (online)
Journal homepage : https://jurnal.fp.unila.ac.id/index.php/JTP

Assessment of Flood Discharge Using the HSS SCS–CN Method and Implications for Adaptive Sabo Dam Design in the Saluki River

Yosephina Puspa Setyoasri[1,✉], Dantje Kardana Natakusumah[2], Vika Febriyani[1], Deddy Irwansyah[1]

[1] Water Resources Management, Faculty of Civil and Environmental Engineering, Institut Teknologi Bandung (ITB), INDONESIA.

[2] Program in Water Resources Management, Faculty of Civil and Environmental Engineering, Institut Teknologi Bandung (ITB), INDONESIA.

Article History:

Received : 15 October 2025
Revised : 17 October 2025
Accepted : 20 December 2025

Keywords:

Curve Number sensitivity,
Flood discharge modeling,
Sabo Dam design,
Saluki River,
SCS–CN synthetic unit hydrograph.

Corresponding Author:
✉ yosephinapuspas@gmail.com
(Yosephina Puspa Setyoasri)

ABSTRACT

In 2018, the Saluki River was morphologically altered due to 7.4 magnitude earthquake. The changes necessitated an evaluation of post-earthquake hydrological conditions prior to Sabo Dam planning. This study aims to estimate the design flood discharge and assess its implications for the preliminary design of a Sabo Dam in Saluki River. Design flood discharge was estimated using the Soil Conservation Service – Curve Number Synthetic Unit Hydrograph (SCS-CN) method. The model results were calibrated using bankfull discharge measured directly. A sensitivity analysis of the CN parameter was performed with ±10% variation to evaluate the effect of post-earthquake changes on peak flood discharge. The design flood discharge was 102.3 m³/s for the 2-year return period (Q_2), 143.9 m³/s (Q_5), 173.7 m³/s (Q_{10}), 212.8 m³/s (Q_{25}), 244.8 m³/s (Q_{50}), and 272.8 m³/s (Q_{100}). The SCS-CN simulation results deviate only 0.15% from the observed bankfull discharge, indicating that the selected hydrological parameters is in agreement with the characteristics of local rainfall-runoff process and catchment areas in the region. The sensitivity test revealed that a 10% increase in the CN value resulted in a 40% increase in the Q_2 peak discharge, while a 10% decrease led to 30% reduction. The Q_{100} discharge of 272.8 m³/s was adopted as the capacity of Sabo Dam design. In conclusion, SCS–CN method remains applicable for watershed conditions analysis in areas which its morphological changes affected by earthquakes. However, the reliability of the model is constrained by limited field observations and potential uncertainties in CN parameter estimation.

1. INTRODUCTION

The 2018 earthquake in Central Sulawesi induced extensive mass movements across mountainous slopes at 77 locations within Palu City, Sigi Regency, and Donggala Regency (Pasigala area), resulting in widespread landslide activity (Sukatja *et al*., 2021). These slope failures caused soil instability and facilitated debris-flow formation in the upper reaches of the Palu River watershed (Balai Wilayah Sungai Sulawesi III Palu, 2023). Earthquakes can substantially increase the availability of unconsolidated materials, including landslide-derived debris, while simultaneously altering river hydromorphological conditions. Such transformations may significantly modify rainfall–runoff responses (Jin *et al*., 2023). Conversely, several studies have demonstrated that Sabo Dam can effectively reduce peak flood discharge and change erosion–sedimentation patterns within river systems (Nakano *et al*., 2024). Nevertheless, comprehensive study that calibrates the Synthetic Unit Hydrology SCS-CN method against observed bankfull discharge in post-earthquake environments, while simultaneously analyzing the implications for Sabo Dam planning, remain limited. This research is essential to establish a more accurate and adaptive planning framework, particularly in regions where geomorphological and hydrological characteristics have been substantially changed by tectonic activity, such as Sigi Regency, Central Sulawesi.

The Saluki River, a third-order sub-watershed of the Palu River Basin, is characterized by predominantly meandering morphology along the channel and has no baseflow, underlain by highly porous bedrock (Kusumah, 2018). Upstream are prone to slope instability, which may substantially increase sediment delivery to downstream. To mitigate these conditions, Sabo Dam in Saluki River constitutes an important structural infrastructure for managing debris flows and reducing sedimentation. Consistent with the function, Sabo Dam is intended to trap and control sediment transport, and stabilize the riverbed upstream against potential degradation induced by debris-flow activity (Zhao *et al*., 2023).

Sabo technology is designed to retain sediment within upstream production zones, control riverbed level fluctuations, and store sediment in upstream (Takahashi, 2007). The advantages of Sabo systems include: (1) maintain equilibrium in sediment transport between upstream and downstream reaches, and (2) sustaining the continuity of sediment supply along the river channel to support aquatic ecosystem while improving public safety (Alfianto *et al*., 2021). In contrast to other flood control structures, such as revetments and levees, which are constructed parallel to the river alignment, Sabo Dam is water infrastructure installed across the river channel. Their operating principle focuses on sediment control by trapping, storing, and releasing fine sediment materials, while allowing water flow to pass downstream (Djudi *et al*., 2014).

In this study, discharge calibration was conducted using the bankfull discharge method, which represents the geomorphologically characteristic flow that forms the natural river channel cross-section and generally correlated to floods with a 1- to 2-year return period (Mulvihill *et al*., 2009). This approach is widely used in areas without streamflow monitoring stations, to validate estimated design discharge (Mouri *et al*., 2013). In this study, the HSS SCS-CN method was employed to estimate flood discharge, as it effectively captures morphological alterations and surface condition changes induced by earthquake events through the Curve Number (CN) parameter. This method has been extensively applied for flood estimation, particularly in regions with dynamic land cover and climatic variability, enabling the evaluation of how parameter changes influence hydrological responses using CN parameter (Sun & Liu, 2025). An increase in the Curve Number (CN), resulting from vegetation loss or the expansion of impervious areas, can significantly elevate peak flood discharge (Shrestha *et al*., 2021). Consequently, conducting a CN sensitivity analysis is critical for evaluating how variations in land cover, soil type, soil permeability, and slope gradient affect flood discharge and their implications for Sabo Dam design (Kousari *et al*., 2010).

The objectives of this study are to estimate the design flood discharge of Saluki River using the HSS SCS–CN method, conduct a Curve Number (CN) sensitivity analysis with a ±10% variation to evaluate its effect on peak discharge (Hosseini & Mahjouri, 2018), and assess the reliability of the estimated discharge through calibration against bankfull discharge, which represent actual field conditions. The study further examines the implications of these design discharge for planning the storage capacity of Sabo Dam in Saluki River. This study uniquely integrates hydrological calibration using bankfull discharge with CN sensitivity analysis to support adaptive Sabo Dam design in post-earthquake environments.

2. MATERIALS AND METHODS

2.1. Materials

Research was performed in Saluki Watershed in Gumbasa Subdistrict, Sigi Regency, Central Sulawesi Province (Figure 1). Administratively, the catchment area included majority of Gumbasa, Lindu, and Palolo Subdistricts. The Saluki Watershed is characterized by catchment area (A) of 62.08 km^2, length (L) of 19.44 km, average land slope (S) of 0.5779%, and centroidal flowpath (Lc) of 10.63 km. Based on soil type data in the Saluki Watershed (Figure 2), the soil type is dominated by clay comprising of 59.01 km^2 (95.05%). The rest is sandy clay loam involving of 3.07 km^2 (4.95%). Based on land cover data (Figure 2), the Saluki Watershed is composed of primarily and secondary dryland forests, built up or settlement areas, dryland agriculture, shrubs, river, and other as detailed in Table 1. Based on land cover and soil type data (Figure 2), the corresponding CN and impervious values for the Saluki Watershed were 76.81 and 5.27, respectively (Table 1).

The materials required for this study include a number of data sets and maps. Table 2 details the types, availability, and sources of data required in this study.

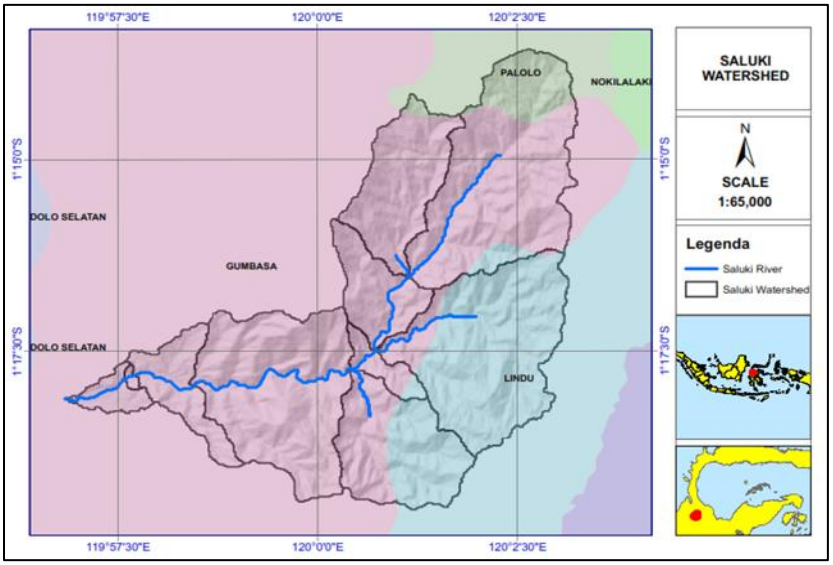

Figure 1. Map of Saluki Watershed

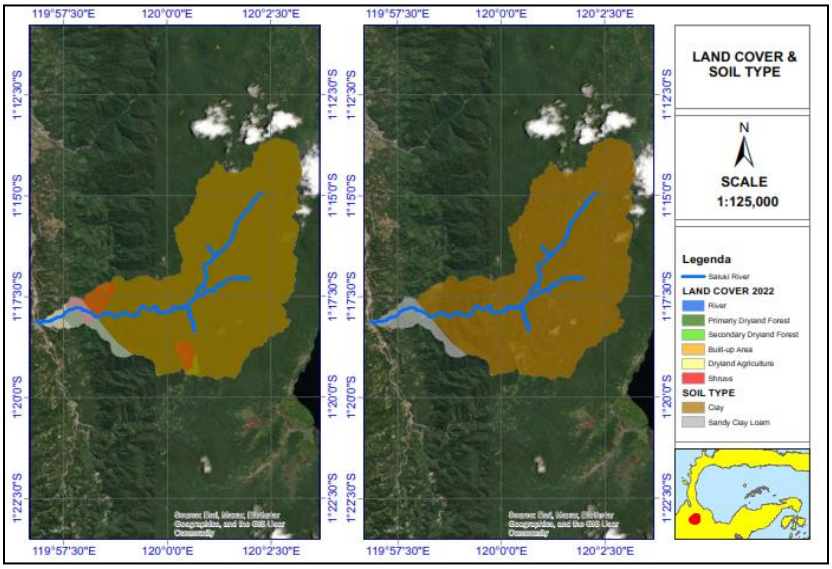

Figure 2. Land cover and soil type of Saluki Watershed

Table 1. Land cover composition, Hydrologic Soil Group (HSG), CN, and Impervious values of Saluki Watershed

Land Cover	Area (A)		HSG	CN	Imp	CN×A	Imp×A	Comp CN	Comp Imp
	(km²)	(%)							
Primarily Dryland Forest	56.50	91.00	D	77	5	4350.22	282.48	76.81	5.27
Primarily Dryland Forest	1.44	2.32	C	70	5	100.828	7.20		
Secondary Dryland Forest	0.29	0.47	D	77	5	22.4138	1.46		
Built-up Area	0.02	0.03	C	90	30	1.78659	0.60		
Dryland Agriculture	0.74	1.19	C	76	5	55.8738	3.68		
Shrubs	2.19	3.53	D	77	5	168.46	10.94		
Shrubs	0.75	1.21	C	70	5	52.4346	3.75		
River	0.02	0.03	D	100	100	2.1857	2.19		
River	0.15	0.24	C	100	100	14.7542	14.75		
Total	62.09	100.0				4768.96	327.04		

Table 2. Type, availability, and source of data required for this study

No.	Data Type	Availability	Data Source
1.	Saluki River Watershed Digital Elevation Model (DEM)	National DEM	DEMNAS (BIG)
2.	Daily Rainfall	Tuva and Tanah Harapan/Palolo Rainfall Stations (2004–2023)	BWS Sulawesi III Palu
3.	Saluki River Geometry	2024 Lidar Measurements	BWS Sulawesi III Palu
4.	Land Use	2022 Land Use Map	Ministry of Environment and Forestry, Indonesia
5.	Soil Type	2022 Soil Map	BWS Sulawesi III Palu
6.	Observation Discharge	Field Observation using current meter	Field Observation

2.2. Research Method Flowchart

The research procedure comprises several key steps: data collection, hydrological analysis, Curve Number (CN) sensitivity analysis with a ±10% variation, calibration using the bankfull discharge approach, and an assessment of the implications of the design flood discharge for Sabo Dam planning, as shown in Figure 3.

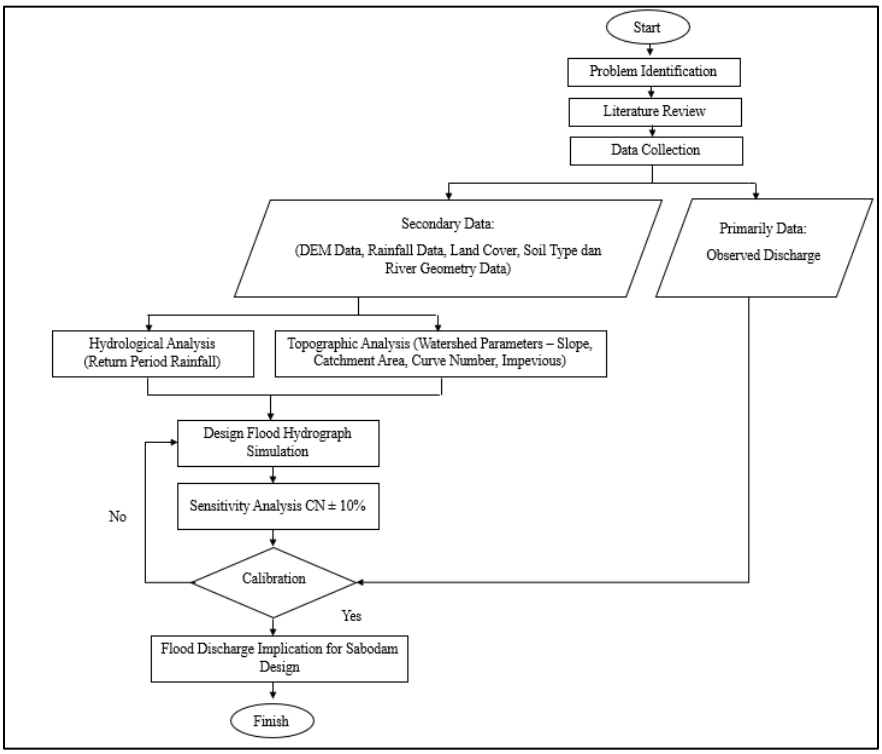

Figure 3. Flowchart for research methods and stages

2.3. Hydrological Analysis

Hydrological analysis was conducted after outlier testing on the rainfall data. The main steps included design rainfall analysis using the Gumbel method, regional design rainfall estimation using the Thiessen polygon method combined with the Area Reduction Factor (ARF), determination of effective rainfall, calculating the design flood discharge, and calibrating flood discharge using bankfull approach. Maximum rainfall data were obtained from two nearby stations, Tuva Station and Tanah Harapan/Palolo Station. Outlier testing was performed to identify both upper and lower outliers, determining whether any data point deviated significantly from the rest of the dataset, either unusually high or low (Layaliya, 2025). This procedure ensures that no rainfall data points are anomalously different from the overall dataset (Robot *et al*., 2014).

Rainfall data were analyzed to determine their frequency characteristics, and distribution estimates were subsequently computed using the Gumbel method. This extreme value distribution is widely employed in hydrology to represent annual peak flood events, particularly in datasets exhibiting negligible skewness (Gumbel, 1941). The results of the frequency analysis were then assessed for goodness-of-fit using both the Chi-Square and Kolmogorov-Smirnov tests. The computation of the Gumbel distribution involves several essential parameters, including the reduced variate, reduced mean, and reduced standard deviation. The corresponding mathematical expressions are presented in Equations (1) – (3).

$$x_{tr} = \bar{x}\frac{y_t + y_n}{Sn}\, s \tag{1}$$

$$k = \frac{y_t + y_n}{Sn} \tag{2}$$

$$y_t = -\ln(-ln\frac{T-1}{T}) \tag{3}$$

where x_{tr} is rainfall at return periode, $\bar{x}$ is mean of the annual peak rainfall, s is standard deviation of the rainfall data, k is probability factor, y_n is reduced mean, which depends on the number of observations (n), S_n is reduced standard deviation, also depending on the number of observations, and y_t is reduced variate, where n represents the sample size, and T is the rainfall return period (Gumbel, 1941).

The Chi-Square test assumes that the observed rainfall data represent a random variable and evaluates their conformity to a theoretical distribution by reference to a Chi-Square probability distribution with degrees of freedom equal to $kp - 1$, where p denotes the number of parameters estimated from the dataset. The test statistic is computed as a weighted sum of squared differences between observed and theoritical values, which are grouped into predefined class intervals. The goodness-of-fit of the Gumbel distribution evaluated using the Chi-Square test is defined in Equation (4) (Kozak, 2025).

$$\chi^2_{i=1} = \sum\frac{(O_i - E_i)^2}{E_i} \tag{4}$$

where χ is the calculated Chi-Square test statistic, k is number of class intervals, O_i is observed frequency in the i^{th} class interval, and E_i is the expected frequency in the i-th class interval.

The Kolmogorov–Smirnov test is a non-parametric goodness-of-fit test, as it does not assume any specific underlying probability distribution. The Kolmogorov–Smirnov test statistic is expressed in Equation (5) (Massey, 1951).

$$Dn = max|\, P(x) \; - \; P0\,(x)| \tag{5}$$

where Dn is the maximum vertical distance between the empirical and theoretical cumulative distribution functions, $P(x)$ is the maximum vertical distance between the empirical and theoretical cumulative distribution functions, and $P0(x)$ is cumulative probability derived from the theoretical distribution.

Areal rainfall (P) was estimated using the Thiessen Polygon method. This method converts point rainfall measurements into areal rainfall values by applying a weighted averaging approach based on the area of influence of each rain gauge. The Thiessen Polygon formulation can be expressed as follows (Triatmodjo, 2008):

$$P = \frac{A_1P_1 + A_2P_2 + A_3P_3 + \cdots + A_nP_n}{A_1 + A_2 + \cdots + A_n} \tag{6}$$

where P_1, P_2, …, P_n is rainfall data at station 1, 2, …, n; and A_1, A_2, …, A_n is the area of influence represented by stations 1, 2, …, n.

2.4. SCS–CN Method

The SCS–CN method was selected due to its robustness in ungauged watersheds and its sensitivity to land-use changes, which are critical under post-earthquake conditions. Data required for flood discharge analysis using SCS–CN involved (Natakusumah *et al*., 2011):

1. Watershed characteristics: The physical characteristics of the watershed include watershed area, slope basin, river length, and centroidal flowpath.
2. Peak time (T_p) and Base time (T_b) :

$$T_L = C_t\,(L\,x\,L_c\,)n \tag{7}$$

$$T_p = (\frac{T_r}{2} + T_L) \tag{8}$$

$$\text{Tb} = 5 \text{ x Tr} \tag{9}$$

where T_L is lag time (hour), C_t is time adjustment coefficient (taken as 1.0), L is river length (km), L_c is centroidal flowpath (km), n = 0.3, and T_r is effective rainfall duration (Natakusumah *et al*., 2011).

3. Peak discharge (Q_p) :

$$Q_p = \frac{(0.2083 \times A)}{T_p} \tag{10}$$

where Q_p is peak discharge (m³/s), A is catchment area (km²), and T_p is peak time (hour) (Sari *et al*., 2020).

2.5. Curve Number (CN) Sensitivity Analysis ± 10%

The Curve Number (CN) in SCS–CN method represents the infiltration capacity of the soil and the degree of impervious surface in a catchment area. CN values are primarily controlled by soil type, land cover, and initial moisture conditions (Cantik *et al*., 2022).

The ±10% CN sensitivity analysis represents a conservative approach that is commonly adopted to simulate potential changes in land-cover conditions. In this study, the analysis was conducted to evaluate the extent to which variations in CN, resulting from alterations in watershed characteristics induced by seismic activity, may influence flood discharge. The selection of the ±10% variation range is based on previous studies by Hosseini & Mahjouri (2018) and Lai *et al*. (2020). These studies indicate that a ±10% change in CN can significantly affect surface runoff simulation results, leading to variations of approximately 25–40% (Verma & Verma, 2023).

2.6. Calibration Using the Bankfull Discharge Approach

Bankfull discharge is defined as the maximum streamflow that can be accommodated by a river channel before water levels exceed the channel banks or levees. The concept of bankfull discharge reflects the outcome of complex interactions among hydrological, geomorphological, and climatological processes Empirical studies have shown that bankfull discharge is typically associated with peak flows characterized by a recurrence interval of approximately 1.5–2 years (Ahilan *et al*., 2013).

To estimate bankfull discharge, Manning coefficient is required and was derived based on observed discharge. Observations were conducted at four representative cross-sections along the river, covering upstream, midstream, and downstream reaches. At each location, discharge observations were repeated three times to capture low-flow, normal-flow, and high-flow conditions. Manning's coefficients (n) obtained from field observations was validated by comparing with standard reference from Ven Te Chow (Chow, 1959). The bankfull discharge was calculated using the Manning equation, which relates river capacity to hydraulic roughness, cross-sectional geometry, and slope.

$$Q = \frac{1}{n} A R^{2/3} S^{1/2} \tag{11}$$

where Q is bankfull discharge (m³/s), n is Manning coefficient, A is flow area (m²), R is hydraulic radius (m), and S is slope (Chow, 1959). Values for n, A, R, and S were derived from direct field observations. The measured bankfull discharge was compared with the peak discharge Q_2, and error value was calculated using the Equation (12).

$$\text{Error} = \frac{|Q_{Bf} - Q_2|}{Q_{Bf}}\ x\ 100\ \% \tag{12}$$

where Q_{Bf} is bankfull discharge (m³/s), and Q_2 peak discharge in 2 year return period (m³/s).

3. RESULTS AND DISCUSSION

3.1. Hydrological Analysis

The rainfall data used in this study consist of annual maximum rainfall records obtained from the Tuva Station and the Tanah Harapan/Palolo Station. The dataset spans the period from 2004 to 2023, covering 20 years of observations, in accordance with the requirements of SNI 2415:2016. The first step of the hydrological analysis involved examining the rainfall data to ensure that they were free from outliers or anomalous values (Figure 4). Using Polygon Thiessen method (Figure 5), weighting coefficients were derived to calculate the areal rainfall corresponding to selected return periods for the Saluki Watershed, as presented in Table 3 and 4.

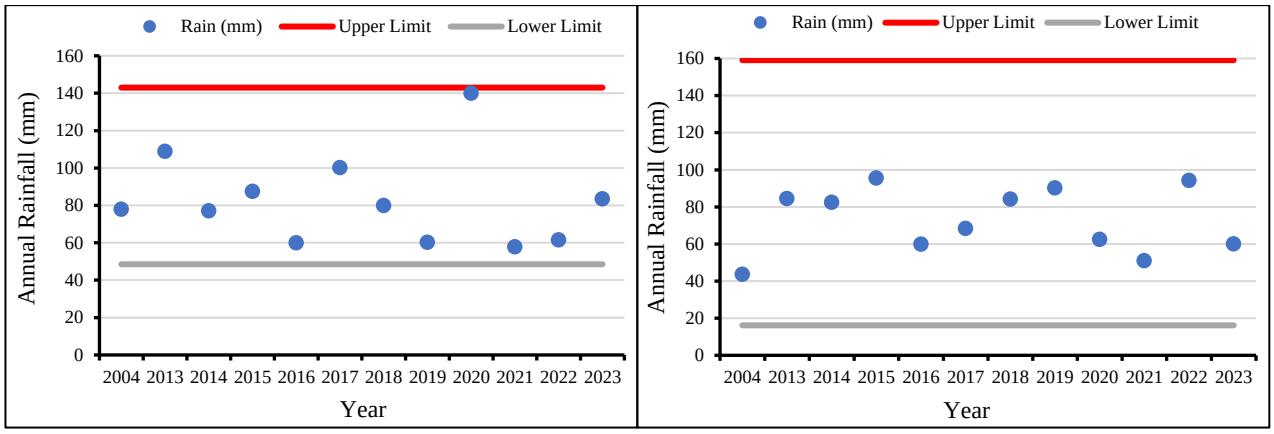

(a) (b)

Figure 4. Outlier analysis of rainfall data for: (a) Tuva Station, and (b) Tanah Harapan Station

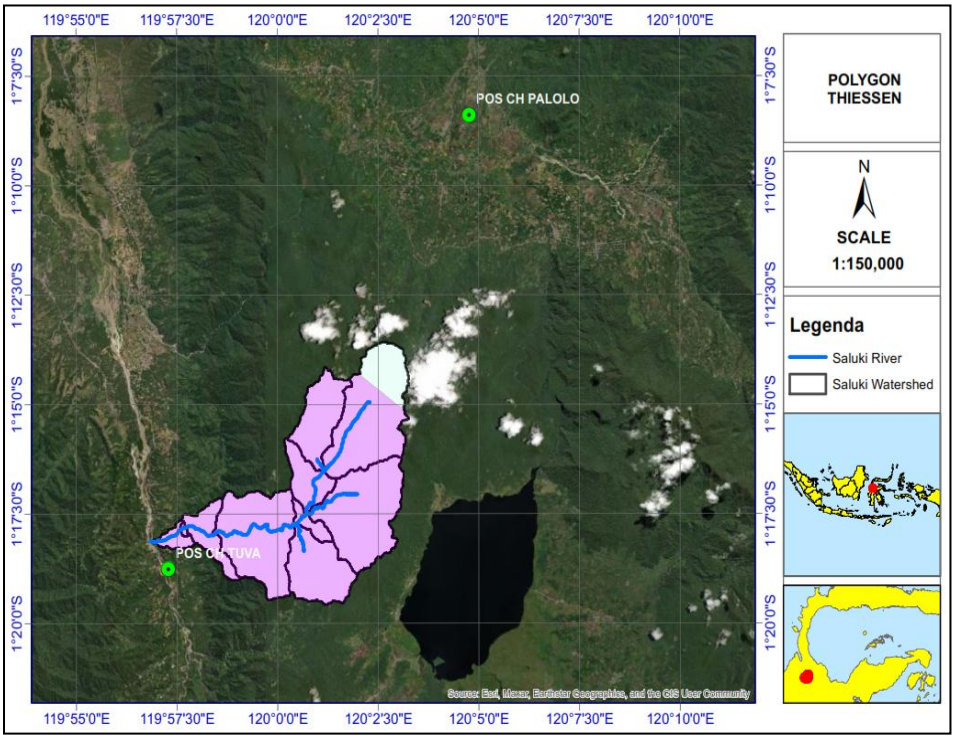

Figure 5.Polygon Thiessen to calculate areal rainfall in Saluki Watershed

Table 3. Thiessen coefficient (TC)

Rainfall Station	Area (km²)	TC
Tuva Station	58.07	0.94
Tanah Harapan Station	4.02	0.06
Total	62.09	1.00

Table 4. Areal rainfall based on return period (*Tr*) using Gumbel method

Tr	Tuva TC = 0.935	Tanah Harapan TC = 0.065	Total TC = 1.000	ARF 0.931
2	82.10	52.13	80.16	74.62
5	99.57	74.47	97.94	91.18
10	111.14	89.26	109.72	102.14
25	125.75	107.95	124.60	115.99
50	136.59	121.81	135.64	126.27
100	147.36	135.57	146.59	136.47

3.2. SCS-CN

The SCS-CN measurement using HEC-HMS 4.11 was performed through the following steps: (1) Construct the basin model; (2) Specify the loss method, applying the SCS Curve Number (CN); (3) Select the transform method, using the SCS Unit Hydrograph; (4) Develop the meteorological model by inputting design rainfall; (5) Set control specifications, including the analysis period (7 days in this study); and (6) Run the simulation model.

Based on the design flood hydrograph analysis, the peak discharge (Qp) is observed to increase with the return period. The peak discharge for the 2-year return period (Q_2) is approximately 102.3 m³/s, while for the 100-year return period (Q_{100}) it reaches about 272.8 m³/s, with intermediate return periods showing a consistent increasing trend. The time to peak is relatively consistent across all return periods, occurring at approximately the 8th hour. Peak discharge reflects the influence of design rainfall intensity on the watershed runoff response. These peak discharge values are subsequently used as a basis for further analysis, particularly in the preliminary study for sabo dam design. The complete results are presented in the figure 6 and table 5, which illustrate the relationship between return period and the resulting peak discharge.

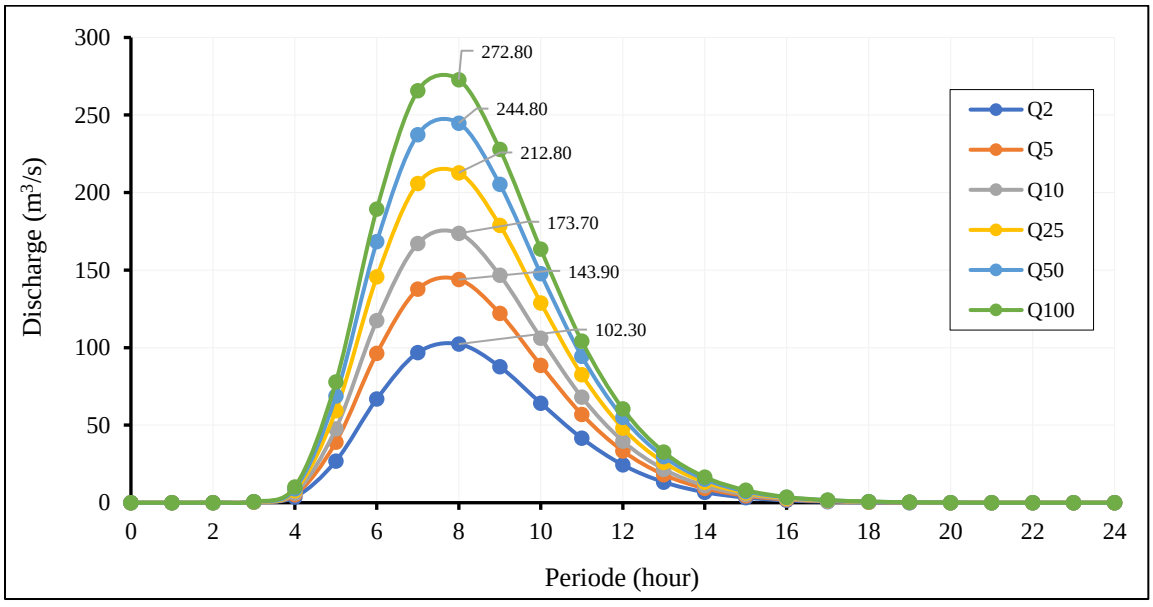

Figure 6. Flood discharge based on HSS SCS for DAS Saluki under different return periods

3.3. CN Sensitivity Analysis (±10%)

Three scenarios were considered: the base CN (SCS–CN), CN increased by 10% (SCS–CN+10), and CN decreased by 10% (SCS–CN–10). Each scenario was simulated for design discharge with 2-year and 100-year return periods as shown in figure 7. This analysis was conducted to assess the impact of CN variations on flood discharge, particularly in earthquake-affected watershed areas. The earthquake induced slope morphological changes and an increase in landslide-affected areas, potentially increasing CN values due to exposed soil and reduced vegetation cover, particularly along rivers in Central Sulawesi (Putranto *et al*., 2024). CN sensitivity analysis is critical as it integrates for potential changes in CN values resulting from earthquakes, allowing estimated design flood discharge for dam planning becomes adaptive post-disaster conditions. The CN adjustments are applied globally to represent overall post-earthquake physical changes, rather than through detailed modifications of land cover.

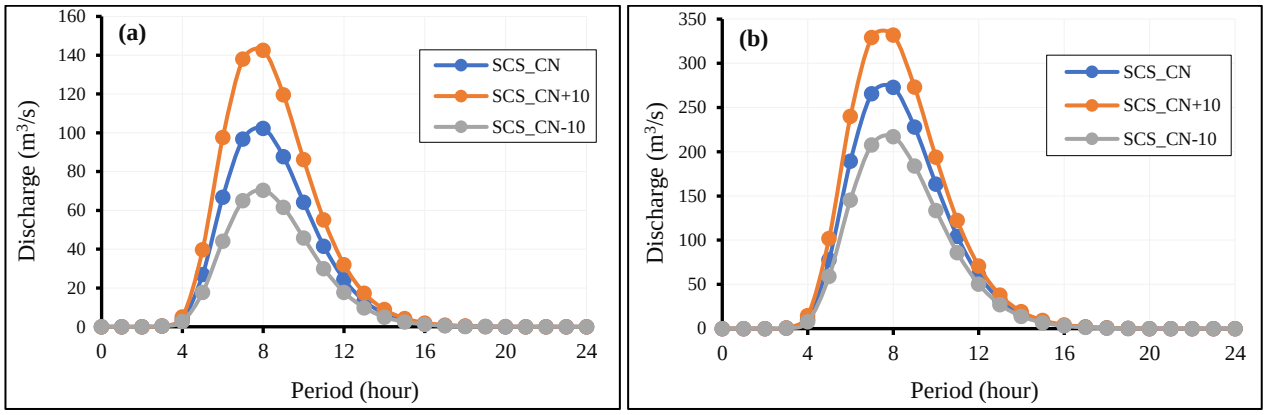

Figure 7. Hydrograph based on three method and two different return period: (a) 2-year return period; (b) 100-year return period

For the 2-year design flood scenario, increasing the CN by 10% led to an approximately 40% rise in peak discharge relative to the baseline CN. The resulting hydrograph displays a steeper peak with a shorter time to reach it. In contrast, reducing CN by 10% produces lower peak flows, reflecting enhanced infiltration due to more permeable soils or denser vegetation cover. In extreme condition with a 100-year return period, the hydrographs exhibit similar overall patterns but differ significantly in peak discharge. The highest peak, approximately 332 m³/s, occurs under the CN+10% scenario, followed by the base CN at around 273 m³/s, and the CN–10% scenario at approximately 217 m³/s.

The increase in peak discharge under higher CN values reflects reduced infiltration capacity and increased surface runoff, which is consistent with post-earthquake land degradation. The nonlinear response between CN variation and peak discharge indicates high model sensitivity, suggesting that small errors in CN estimation may lead to significant uncertainty in design discharge.

3.4. Bankfull Discharge Calibration

Estimating bankfull discharge requires Manning coefficient, which was derived from field observation. Observations were conducted at four representative cross-sections along the river, covering upstream, midstream, and downstream reaches, as shown in Figure 8. At each location, flow observations were repeated three times to capture low-, normal-, and high-flow conditions. Manning coefficients from observation was validated against standard values reported in Chow (1959). Based on the three flow conditions (Table 5-7), the average of Manning coefficient can calculated as n = 0.0306.

Bankfull discharge was calibrated by comparing the estimated bankfull discharge with the peak discharge corresponding to a 2-year return period. Following the calculations, bankfull discharge at Sections 1, 2, 3, and 4 was determined as 102.40, 102.69, 102.20, and 102.52 m³/s, respectively, yielding an average bankfull discharge of 102.45 m³/s for calibration (Table 8). The bankfull discharge was determined by rating curve at each measurement site, relating observation discharge to channel depth as presented in Figure 9.

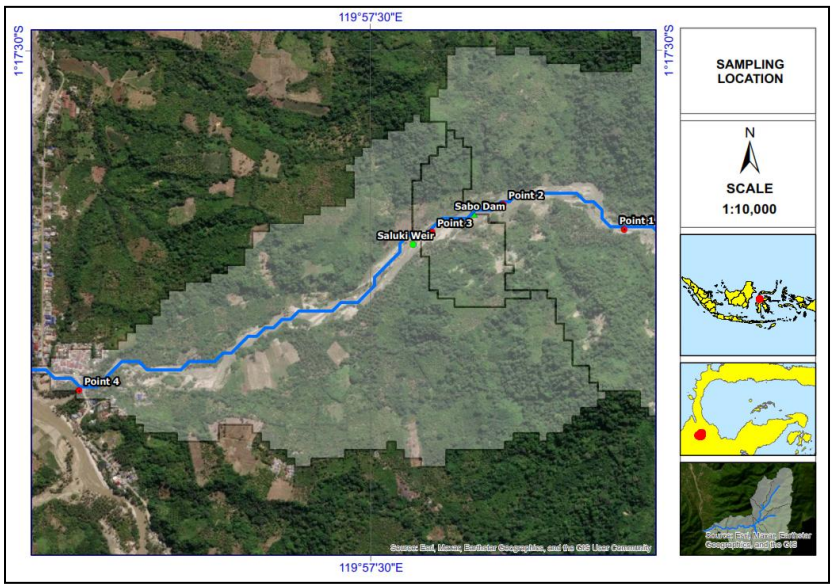

Figure 8. Four sampling location representing upstream, midstream, and downstream of Saluki Watershed

Table 5. Observation in normal flow

1st Observation							
Point	**Q (m³/s)**	**A (m²)**	**v (average) (m/s)**	**P (m)**	**R (m)**	**S**	**n**
1	1.75	1.84	0.95	20.92	0.09	0.03	0.04
2	1.92	1.52	1.26	17.5	0.09	0.02	0.02
3	1.16	1.99	0.58	19.91	0.1	0.02	0.05
4	0.75	0.9	0.84	9.74	0.09	0.01	0.02
			Average				0.034

Table 6. Observation in high flow

2nd Observation							
Point	**Q (m³/s)**	**A (m²)**	**v (average) (m/s)**	**P (m)**	**R (m)**	**S**	**n**
1	2.11	1.7	1.24	19.01	0.09	0.03	0.03
2	2.22	1.67	1.33	17.04	0.1	0.02	0.02
3	1.97	1.88	1.05	20.1	0.09	0.02	0.03
4	1.12	1.11	1	10.78	0.1	0.01	0.02
			Average				0.028

Table 7. Observation in low flow

3rd Observation							
Point	**Q (m³/s)**	**A (m²)**	**v (average) (m/s)**	**P (m)**	**R (m)**	**S**	**n**
1	1.61	1.65	0.98	19.21	0.09	0.03	0.03
2	1.67	1.53	1.09	17.5	0.09	0.02	0.03
3	1.62	1.52	1.06	17.61	0.09	0.02	0.03
4	1.28	1.14	1.12	12.09	0.09	0.01	0.02
			Average				0.029

Table 8. Calibration of design flood discharge against bankfull discharge

Calibration	**Q bankfull**	**SCS_CN**	**SCS_CN+10%**	**SCS_CN-10%**
Q_2	102.45	102.30	142.60	70.40
Deviation		0.15	40.15	32.05
Error		0.15%	39.18%	31.29%

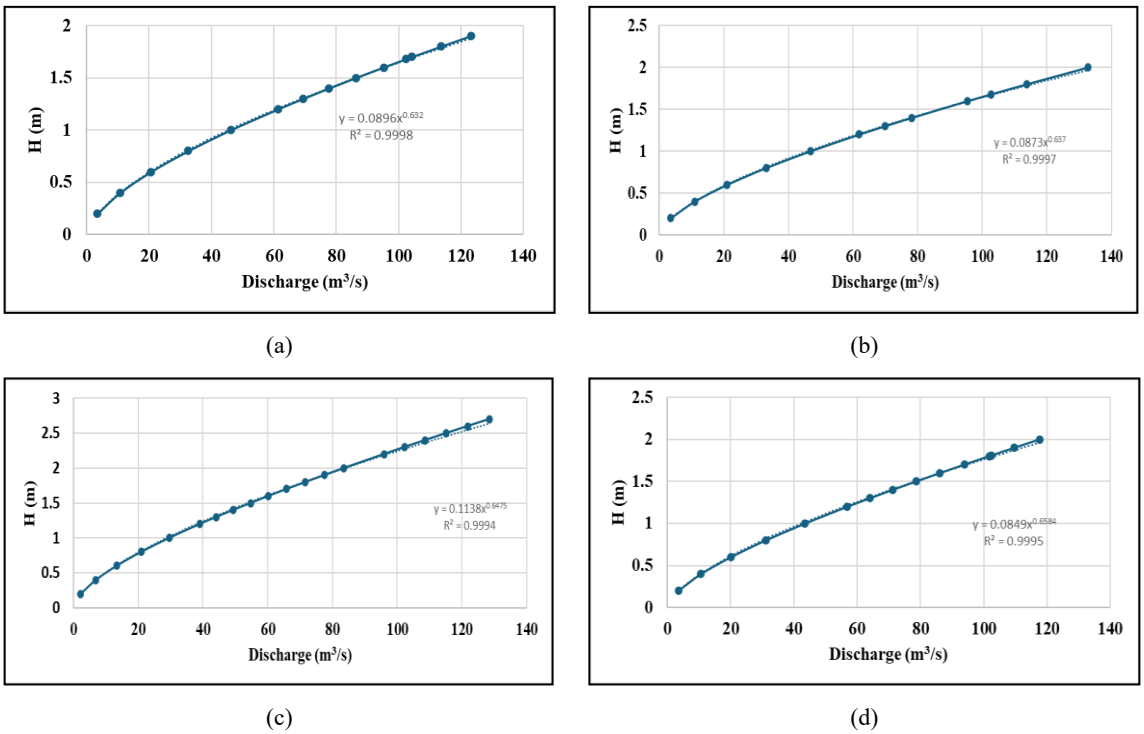

Figure 9. Rating curve for four sampling points: (a) Point 1, (b) Point 2, (c) Point 3, (d) Point 4

3.5. Implications for Sabo Dam Design

The Curve Number (CN) sensitivity analysis and calibration against bankfull discharge describe the relation between watershed hydrological characteristics and Sabo Dam capacity. CN values represent surface infiltration and land cover conditions, which influence runoff and consequently, debris flood and sediment transport to the river system. Calibration of CN against bankfull discharge not only evaluates the accuracy of the hydrological model but also serves as parameters for designing safe and efficient Sabo Dam structures.

A 10% rise in CN relative to the baseline leads to an approximate 40% increase in peak discharge, whereas a 10% reduction in CN lowers the peak discharge by approximately 30%. Elevated CN values indicate reduced infiltration capacity and higher surface runoff volume, which potentially transporting greater sediment loads downstream.

In a Sabo Dam structure, an increase in CN implies a reduced Sabo Dam lifespan, as sediment accumulates faster than the design capacity. Consequently, the Sabo Dam in the Saluki watershed should be designed with sufficient sediment storage and a bottom outlet to facilitate the removal of excess material.

This study has several limitations. First, the calibration relies on limited field observations from four cross-sections, which may not fully represent spatial variability along the river. Second, the CN parameter was adjusted uniformly across the watershed, which may oversimplify actual heterogeneous land-cover changes. Third, the absence of long-term discharge monitoring data restricts validation of model performance under extreme conditions.

4. CONCLUSIONS

The study indicates that the design flood discharge for the Saluki watershed are Q_2 = 102.3 m³/s, Q_5 = 143.9 m³/s, Q_{10} = 173.7 m³/s, Q_{25} = 212.8 m³/s, Q_{50} = 244.8 m³/s, and Q_{100} = 272.8 m³/s. High CN values tend to overestimate surface runoff and peak discharge, whereas low CN values may reduce the accuracy of bankfull discharge estimations. This study highlights the reliability of HSS SCS-CN calibration in capturing the hydrological response of the Saluki River following the earthquake, providing a basis for adaptive and sustainable dam design parameters. This approach would

offer a more realistic depiction of post-earthquake hydrological conditions and facilitate an optimal assessment to guide adaptive Sabo Dam design in response to changes in watershed characteristics. Future studies should incorporate larger datasets and distributed parameter approaches to improve model robustness and reduce uncertainty in flood estimation.

AUTHOR CONTRIBUTION STATEMENT

Author	C	M	So	Va	Fo	I	R	D	O	E	Vi	Su	P	Fu
YPS	✓	✓	✓	✓		✓			✓	✓	✓			
DKN										✓	✓			
VF									✓	✓				
WM						✓	✓							

C: Conceptualization	Fo: Formal Analysis	O: Writing - Original Draft	Fu: Funding Acquisition
M: Methodology	I: Investigation	E: Writing - Review & Editing	P: Project Administration
So: Software	D: Data Curation	Vi: Visualization	
Va: Validation	R: Resources	Su: Supervision	

REFERENCES

Ahilan, S., O'Sullivan, J.J., Bruen, M., Brauders, N., & Healy, D. (2013). Bankfull discharge and recurrence intervals in Irish rivers floods. *Proceedings of the ICE – Water Management,* ***166***(7), 381–393. https://doi.org/10.1680/wama.11.00078

Alfianto, A., Cecilia, S., Hidayah, A.N., Anjelita., & Sukatja, C.B. (2021). Perencanaan sabo untuk mengendalikan laju sedimentasi di Rawapening. *Jurnal Sumber Daya Air,* ***17***(1), 1-12. https://doi.org/10.32679/jsda.v17i1.610

Balai Wilayah Sungai Sulawesi III Palu. (2023). *Pola pengelolaan sumber daya air wilayah Sungai Palu–Lariang.* Kementerian Pekerjaan Umum dan Perumahan Rakyat.

Cantik, B.K.P., Sapan, E.G.A., Ghiffari, M.R.A., Yuvhendmindo, M.R., & Aziz, M.L. (2022). Surface runoff analysis using SCS-CN method in Summarecon Serpong area. *INERSIA Informasi dan Ekspose Hasil Riset Teknik Sipil dan Arsitektur,* ***18***(2), 94–103. https://doi.org/10.21831/inersia.v18i2.53248

Chow, V.T. (1959). *Open-Channel Hydraulics*. McGraw-Hill.

Djudi, D., Hassan, C., Soewarno, S., Yunita, F.T., & Gardiawan, G.R. (2014). *Stabilitas Pondasi Mengambang Sabodam (Kegiatan Litbang)* (Issue 022). Pusat Penelitian dan Pengembangan Sumber Daya Air, Kementerian Pekerjaan Umum dan Perumahan Rakyat.

Gumbel, E.J. (1941). The return period of flood flows. *The Annals of Mathematical Statistics,* ***12***(2), 163–190. https://www.jstor.org/stable/2235766

Hosseini, S.M., & Mahjouri, N. (2018). Sensitivity and fuzzy uncertainty analyses in the determination of SCS-CN parameters from rainfall–runoff data. *Hydrological Sciences Journal,* ***63***(3), 457–473. https://doi.org/10.1080/02626667.2018.1437272

Jin, W., Cui, P., Zhang, G., Wang, J., Zhang, Y., & Zhang, P. (2023). Evaluating the post-earthquake landslides sediment supply capacity for debris flows. *CATENA,* ***220***, 106649. https://doi.org/10.1016/j.catena.2022.106649

Kousari, M.R., Malekinezhad, H., Ahani, H., & Asadi Zarch, M.A. (2010). Sensitivity analysis and impact quantification of the main factors affecting peak discharge in the SCS curve number method: An analysis of Iranian watersheds. *Quaternary International,* ***226***(1–2), 66–74. https://doi.org/10.1016/j.quaint.2010.05.011

Kozak, K. (2021). *Statistics Using Technology* (2nd ed.). Coconino Community College. Lulu.com. ISBN: 9781329757257

Kusumah, A.W., Solikhin, A., Andiani, Anjar, H., Omang, A., Soehami, A., Cipta, A., Defrizal, Yuwana, D.A., Firdaus, E.R., Fadli, Djunursyah, G.M.L., Hasibuan, G., Afif, H., Santosa, I., P., I.E., Sulistyawan, I.H., Kurniah, Falah, N., … Yunara, D.T. (2018). *Di Balik Pesona Palu: Bencana Melanda, Geologi Menata*. Badan Geologi, Kementerian Energi dan Sumber Daya Mineral.

Layaliya, H.N. (2025). Kajian morfologi sungai akibat bangunan pengendali sedimen dan river improvement di Sungai Namo Kabupaten Sigi. [*Master's Thesis*], Institut Teknologi Bandung.

Massey, F.J. (1951). The Kolmogorov–Smirnov test for goodness of fit. *Journal of the American Statistical Association,* ***46***(253), 68–78. https://doi.org/10.1080/01621459.1951.10500769

Mouri, G., Golosov, V., Chalov, S., Belyaev, V., Shiiba, M., Hori, T., Shinoda, S., & Oki, T. (2013). Assessing the effects of consecutive sediment-control dams using a numerical hydraulic experiment to model river-bed variation. *CATENA,* ***104***, 174–185. https://doi.org/10.1016/j.catena.2012.11.008

Mulvihill, C.I., Baldigo, B.P., Miller, S.J., DeKoskie, D., & DuBois, J. (2009). *Bankfull discharge and channel characteristics of streams in New York State* (Scientific Investigations Report 2009–5144). U.S. Geological Survey.

Nakano, D., Suzuki, J., Fujita, K., & Imamura, M. (2024). Restoration effects of sediment supply by sediment sluicing dam operations on macroinvertebrate assemblages in the Mimi River, Japan. *Ecological Engineering,* ***206***, 107336. https://doi.org/10.1016/j.ecoleng.2024.107336

Natakusumah, D.K., Hatmoko, W., & Harlan, D. (2011). Prosedur umum perhitungan hidrograf satuan sintetis dengan cara ITB dan beberapa contoh penerapannya. *Jurnal Teknik Sipil*, ***18***(3). https://doi.org/10.5614/jts.2011.18.3.6

Putranto, A.E., Adityawan, M.B., Moerwanto, A.S., & Natakusumah, D.K. (2024). Analysis of the effectiveness of sediment control structures and river improvement on the Omu River post-earthquake in Sigi Regency. *Jurnal Teknik Sumber Daya Air*, ***15***(1). https://doi.org/10.32679/jth.v15i1.749

Robot, J.A., Mananoma, T., Wuisan, E.M., & Tangkudung, H. (2014). Analisis debit banjir Sungai Ranoyapo menggunakan metode HSS Gama-I dan HSS Limantara. *Jurnal Sipil Statik*, ***2***(1).

Sari, A.N.S., Pranoto, R., & Suryan, V. (2020). Perhitungan hidrograf banjir dengan metode hidrograf satuan sintesis SCS (Soil Conservation Service) di Kota Palembang. *Journal of Airport Engineering Technology*, ***1***(1). https://doi.org/10.52989/jaet.v1i1.1

Shrestha, S., Cui, S., Xu, L., Wang, L., Manandhar, B., & Ding, S. (2021). Impact of land use change due to urbanisation on surface runoff using GIS-based SCS–CN method: A case study of Xiamen City, China. *Land*, ***10***(8), 839. https://doi.org/10.3390/land10080839

Sukatja, C.B., W.R., B., & Bahri, P. (2021). Mitigasi dan penanggulangan bencana banjir debris pasca Gempa Palu 2018. *Jurnal Teknik Hidraulik*, ***12***(1). https://doi.org/10.32679/jth.v12i1.648

Sun, Q., & Liu, J. (2025). The impact of rainfall value on the accuracy of the SCS-CN model: Selection of model parameters. *AQUA: Water Infrastructure, Ecosystems and Society*, ***74***(1), 142–158. https://doi.org/10.2166/aqua.2024.288

Takahashi, T. (2007). Debris flow: Mechanics, prediction and countermeasures (1st ed.). Taylor & Francis. https://doi.org/10.1201/9780203946282

Triatmodjo, B. (2008). *Hidrologi Terapan* (Cet. 1). Beta Offset, Yogyakarta. ISBN: 978-979-8541-40-7

Verma, S., & Verma, R.K. (2023). SCS-CN methodology further modified. *Water Supply*, ***23***(6), 2604–2622. https://doi.org/10.2166/ws.2023.129

Zhao, B., Xin, T., Li, P., Ma, F., Gao, B., & Fan, R. (2023). Regulation of flood dynamics by a check dam system in a typical ecological construction watershed on the Loess Plateau, China. *Water*, ***15***(11), 2000. https://doi.org/10.3390/w15112000